Simulate fluid flow in porous media with a probabilistic lattice gas

Lin Zhang

ABSTRACT

Some numerical experiments illustrate the linear and nonlinear behavior of the probabilistic lattice gas model, M2, simulating fluid flow. Numerical methods of implementing the relevant boundary conditions and creating the pressure gradient are derived. As a practical application, I model the fluid flow through a porous medium. The results of our experiments are similar to those obtained by other methods.

INTRODUCTION

Modeling fluid flow in porous media is of interest in both geophysics and petroleum engineering. Many numerical methods have been developed to simulate the fluid flow in such complicated media and to estimate the parameters of the media, for example, permeability. Rothman (1988) discusses a new approach to this problem. He used cellular-automaton fluids as the basis of his model, and developed numerical techniques for implementing the appropriate boundary conditions, creating a pressure gradient, and measuring the permeability. He also studied the scale problem in the simulation and came up with a conclusion that the linear dimension of a void region in the porous media should be about twice the mean free path of a lattice gas particle.

The lattice gas model that Rothman used is FHP, proposed by Frisch et al. (1986). This model, like many other ones, describes the individual particle motion. Although the numerical calculation involved in simulating each lattice gas is just simple binary manipulation, the computation time for modeling a physical phenomenon could be very long because many grid points are used. The memory could also be a problem, especially when 3-D models are concerned. One way to overcome these difficulties is to utilize newly developed computer technology, for

example, special-purpose microcomputers or massively parallel machines. In this paper, I present an alternate way. I use the probabilistic lattice gas model M2, proposed by Muir (1987). This model treats the lattice gas as an ensemble and the calculations are carried out on probability values. This feature not only reduces the number of grid points in an experiment by orders magnitude, but also offers an opportunity to take the computational advantages of the conventional computers. Therefore this model may provide saving in time and in space, and opens the door to 3-D simulation.

Muir's algorithm

In SEP-57, I (1988) discussed the numerical methods for M2. My results show that Muir's algorithm gives the same solution as do other methods. Actually, one step of Muir's algorithm can be understood as the collision rule on the probability of the existence of particles. Here I restate Muir's algorithm:

1. The input vector is disassembled into the set of all possible states weighted by their probabilities.
2. Each weighted state is replaced by the weighted average of all the constraint-equivalent states.
3. These weighted average states are reassembled into the output vector.

In the case of the hexagonal lattice, there are three groups of the equivalent states:

$$\begin{array}{lll} \{(101010), & (010101)\} & \\ \{(100100), & (010010), & (001001)\} \\ \{(110110), & (011011), & (101101)\} \end{array} \tag{1}$$

Following is a C-subroutine that does one step of Muir's algorithm.

```
/* this subroutine runs one step of Muir's algorithm on hexgonal M2*/

francis(nvertex,u)
int nvertex;
float *u;
{
   float g1st1, g1st2, g2st1, g2st2, g2st3, g3st1, g3st2, g3st3;
   float est1, est2, est3;

/*compute the probability of equivalent states*/
   g1st1=(1.0-u[0])*u[1]*(1.0-u[2])*u[3]*(1.0-u[4])*u[5];
   g1st2=u[0]*(1.0-u[1])*u[2]*(1.0-u[3])*u[4]*(1.0-u[5]);
   g2st1=(1.0-u[0])*(1.0-u[1])*u[2]*(1.0-u[3])*(1.0-u[4])*u[5];
   g2st2=(1.0-u[0])*u[1]*(1.0-u[2])*(1.0-u[3])*u[4]*(1.0-u[5]);
   g2st3=u[0]*(1.0-u[1])*(1.0-u[2])*u[3]*(1.0-u[4])*(1.0-u[5]);
   g3st1=u[0]*u[1]*(1.0-u[2])*u[3]*u[4]*(1.0-u[5]);
   g3st2=(1.0-u[0])*u[1]*u[2]*(1.0-u[3])*u[4]*u[5];
   g3st3=u[0]*(1.0-u[1])*u[2]*u[3]*(1.0-u[4])*u[5];

/*average the probability*/
   est1=(g1st1+g1st2)/2.0;
   est2=(g2st1+g2st2+g2st3)/3.0;
   est3=(g3st1+g3st2+g3st3)/3.0;
```

```
/*update the probability vector*/
   u[0]+=est1+est2+2.*est3-g1st2-g2st3-g3st1-g3st3;
   u[1]+=est1+est2+2.*est3-g1st1-g2st2-g3st1-g3st2;
   u[2]+=est1+est2+2.*est3-g1st2-g2st1-g3st2-g3st3;
   u[3]+=est1+est2+2.*est3-g1st1-g2st3-g3st1-g3st3;
   u[4]+=est1+est2+2.*est3-g1st2-g2st2-g3st1-g3st2;
   u[5]+=est1+est2+2.*est3-g1st1-g2st1-g3st2-g3st3;
}
```

Boundary conditions

I consider two kinds of relevant boundaries: no-slip boundary and constant pressure boundary. The specific numerical techniques can be worked out by following Rothman's treatment. The no-slip boundary is simulated by letting the probability of the reflected particles be equal to the probability of the incoming particles. The constant pressure boundary is simulated by maintaining a constant increment of the momentum. The total mass is conserved by properly circulating the probability values of the particles. As pointed out in my early paper, the computation involved in the probabilistic lattice gas model is completely deterministic. The behavior of each lattice gas will directly influence the results of the simulation. Thus special care must be taken in order to simulate any phenomenon with certain symmetry.

Assumptions

I restrict my discussion to viscous incompressible fluid flow. I assume that the gravitational force on the fluid is irrelevant, either because the channel is horizontal or because this force is small compared with the forces associated with the pressure gradient. I consider the flow with a relatively wide range of Reynolds number so as to study the transition from the linear flow to the nonlinear flow.

In the following sections, I first show an example of linear flow, namely plane Poiseuille flow. Then I illustrate the nonlinear behavior of the fluid when it passes through an obstacle. Finally the fluid flow through the porous medium is simulated.

LINEAR FLOW

In this section, I discuss the linear flow through a channel formed by two parallel rigid planes. Figure 1 shows the geometry of the experiment. The upper and lower boundaries are no-slip boundaries. At left and right ends, two constant pressures are maintained. I will show that the velocity distribution resulted from the simulation agrees with the theory quite well.

Theory

In the case of small Reynolds number, the viscous forces dominate the inertial forces. The behavior of the flow is approximately linear and can be described by

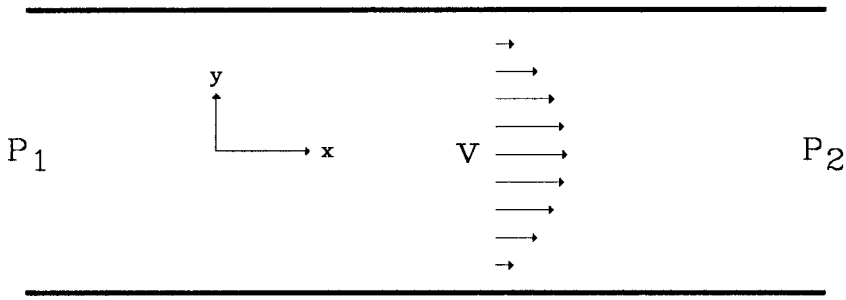

FIG. 1. The configuration of the channel flow experiment. The upper and lower boundaries are no-slip boundaries. The constant pressures are maintained at two ends.

Darcy's law

$$q = \frac{k}{\mu} G, \tag{2}$$

where q is the flow rate, k is permeability of the medium, μ is the viscosity of the fluid and $-G = dP/dx$ is the pressure gradient. From this equation, together with the conservation principle, it is not difficult to derive the horizontal velocity distribution across the channel.

$$v_x = \frac{G}{2\mu}\left(\frac{d^2}{4} - y^2\right), \tag{3}$$

where d is the distance between two plates.

Results

The experiment shown in Figure 1 is conducted with varying parameters. Figure 2, 3 and 4 show the results of the experiment with an array of 64×33 elements. The odd number 33 is chosen for symmetry. The background particle density is uniform with the probability of 0.2 for all six directions. The constant increments of momenta are 0.05 at the entrance and 0. at the exit. Figure 2 plots the total flow rate as the function of time step. We see that, after 400 iterations, the flow reaches the steady state. Figure 3 displays the velocity field in the channel. The flow is horizontal almost everywhere. There are two curves in Figure 4. One is the theoretical data computed from equation (3) and the other is the corresponding data obtained from the experiment. The viscosity μ in equation (3) is an unknown parameter, but it is a scale factor and can be chosen by defining specific units. The coincidence of two curves tells us the accuracy of the model I use. Notice that the horizontal velocities at the boundaries are not exactly zero. This is not unreasonable because the grid points at the boundaries actually represent the average behavior of a group of lattice gas in the neighborhood of the boundaries.

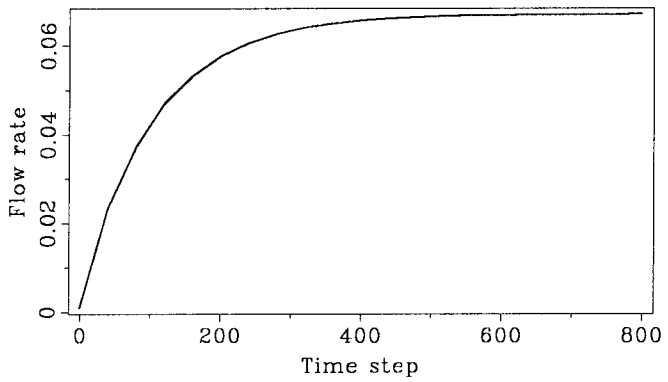

FIG. 2. The flow rate as the function of time step. After about 400 steps, the flow becomes steady.

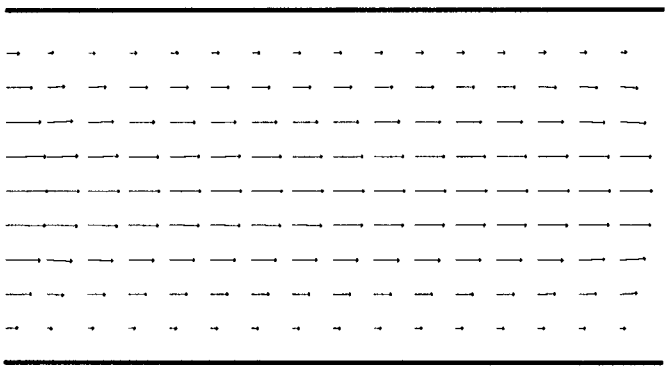

FIG. 3. The velocity field in the channel. The velocity is horizontal everywhere except at the entrance and at the exit.

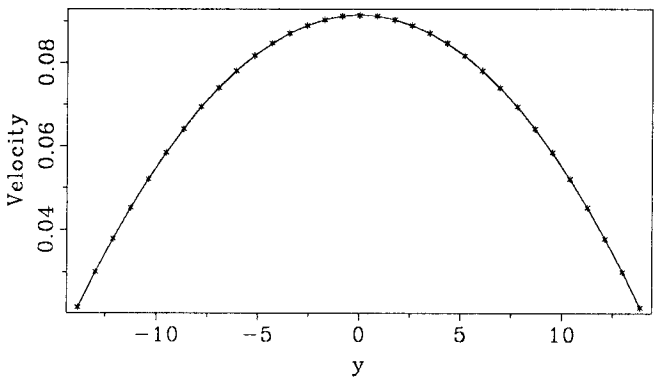

FIG. 4. The continuous line shows the theoretical results of the horizontal velocity distribution across the channel, and the stars indicate the data obtained from the experiment. Good agreement can be seen.

NONLINEAR FLOW

The general behavior of the flow satisfies the incompressible Navier-Stokes equations.

$$\nabla \cdot \mathbf{v} = 0 \tag{4}$$

$$\rho \frac{\partial \mathbf{v}}{\partial t} = -\rho(\mathbf{v} \cdot \nabla)\mathbf{v} - \nabla p + \mu \nabla^2 \mathbf{v}.$$

Frisch (1986) showed that, with the hexagonal lattice gas, the FHP model actually solves the nonlinear equation (4) numerically. Rothman (1988) gave a simple derivation of the equation (4) from the microscopic collision rules that he used. He pointed out that the precise details of the collision rules do not affect the general form of the derived equations, but the value of μ. Therefore it is conjectured that M2 can also solve equation (4) numerically although the collision rule of M2 has the special feature of irreversibility. In the rest part of this paper, I will not discuss the theoretical proof of this conjecture. Instead, I use the numerical experiments to show the qualitative behavior of M2.

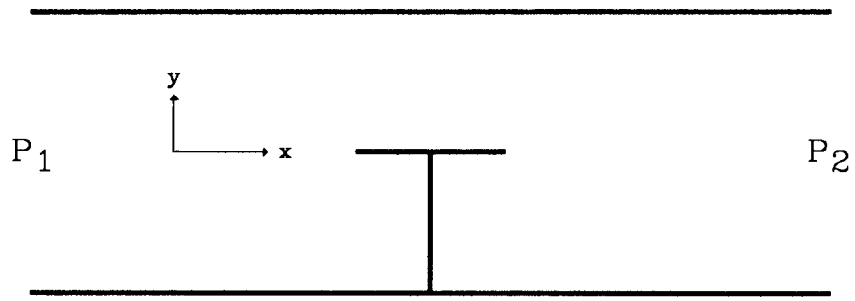

FIG. 5. A T-shape obstacle is set in the channel. All solid lines are no-slip boundaries. A high pressure gradient is created by keeping the constant increments of the momenta at two ends.

Flow past an obstacle

Relative motion between some object and a fluid is common when the porous medium are concerned. To test the nonlinear behaviors of M2 model, an experiment based on geometry shown in Figure 5 is programmed. The size of the lattice array is 64×21. The background particle density is 0.5. The increments of momenta are 0.1 and 0. at two ends respectively. After 800 time steps, the flow becomes steady. Figure 6 shows the velocity field of the flow. The vertices are formed in the shadows of the T-shape obstacle. At the corners of the entrance and the exit, we see the small eddies. To compare the result obtained with different models, I did the same experiment on a linear probabilistic lattice model. The result is also shown in Figure 6. Notice that for the linear model there is no small eddies at the

corners of the two ends. The vertices in the velocity field resulted from the linear model is much more regular than that from the nonlinear model.

Flow in porous media

Another interesting experiment related to the nonlinear flow is to simulate the fluid flow in the two dimensional synthetic porous medium. I use the synthetic pattern generated by Rothman. In my experiment, the array of size 128×64 is divided into many 8×8 subarrays. Each subarray represents either a void space through which the fluid flows, or a rigid space in which there is no fluid flow. The background particle density is 0.5. The pressure gradient is about 2.5 times higher than that of last experiment.

Figure 7 shows the result of this experiment. The velocity field is displayed by arrows. At each location, the length of the arrow represents the amplitude of the velocity and the direction of the arrow points to the direction of the flow. We can see that many features of this velocity field are similar to what Rothman found. The majority of the flow follows several winding paths. There are some dead regions where flow is very slow. The flow velocity increases at the locations where the size of pore decreases. If we plot only the directions of the flow, as we did in Figure 6, many vertices can be identified. The major difference between the Figure 7 and the corresponding figure in Rothman's paper is at the locations near dead regions. The velocity field in Rothman's figure shows that the flow tends to permeate into dead regions. The velocity field in Figure 7 shows that the flow tends to pass away from dead regions. Two possible explanations of this phenomenon are: 1. the model I use may have low viscosity; 2. the effective pressure gradient in my experiment is high.

CONCLUSION

I have investigated the possibility of using the probabilistic lattice gas model to simulate the fluid flow. The results I obtained are quite encouraging. The future work may include the derivation of the Navier-Stokes equations from the model I used and more experiments which explain the phenomena quantitatively.

ACKNOWLEDGMENTS

I would like to thank Francis Muir for many fruitful discussions and suggestions. Thanks also to Joe Delinger for his tutoring on the graphic tools.

REFERENCES

Frish, U., Hasslacher, B., and Pomeau, Y., 1986, Lattice-gas automata for the Navier-Stokes equation: Phys. Rev. Lett., **56**, 1505-1507.

Muir, F., 1987, Three experimental modeling systems: SEP–**51**, 119-128.

Rothman, D. H., 1988, Cellular-automaton fluids: A model for flow in porous media: Geophysics, **53**, 509-518.

Wolfram, S., 1986, Theory and Applications of cellular automata: World Scientific.

Zhang, L., 1988, Simulation of fluid-dynamic processes with a probabilistic lattice gas: SEP–**57**, 259-277.

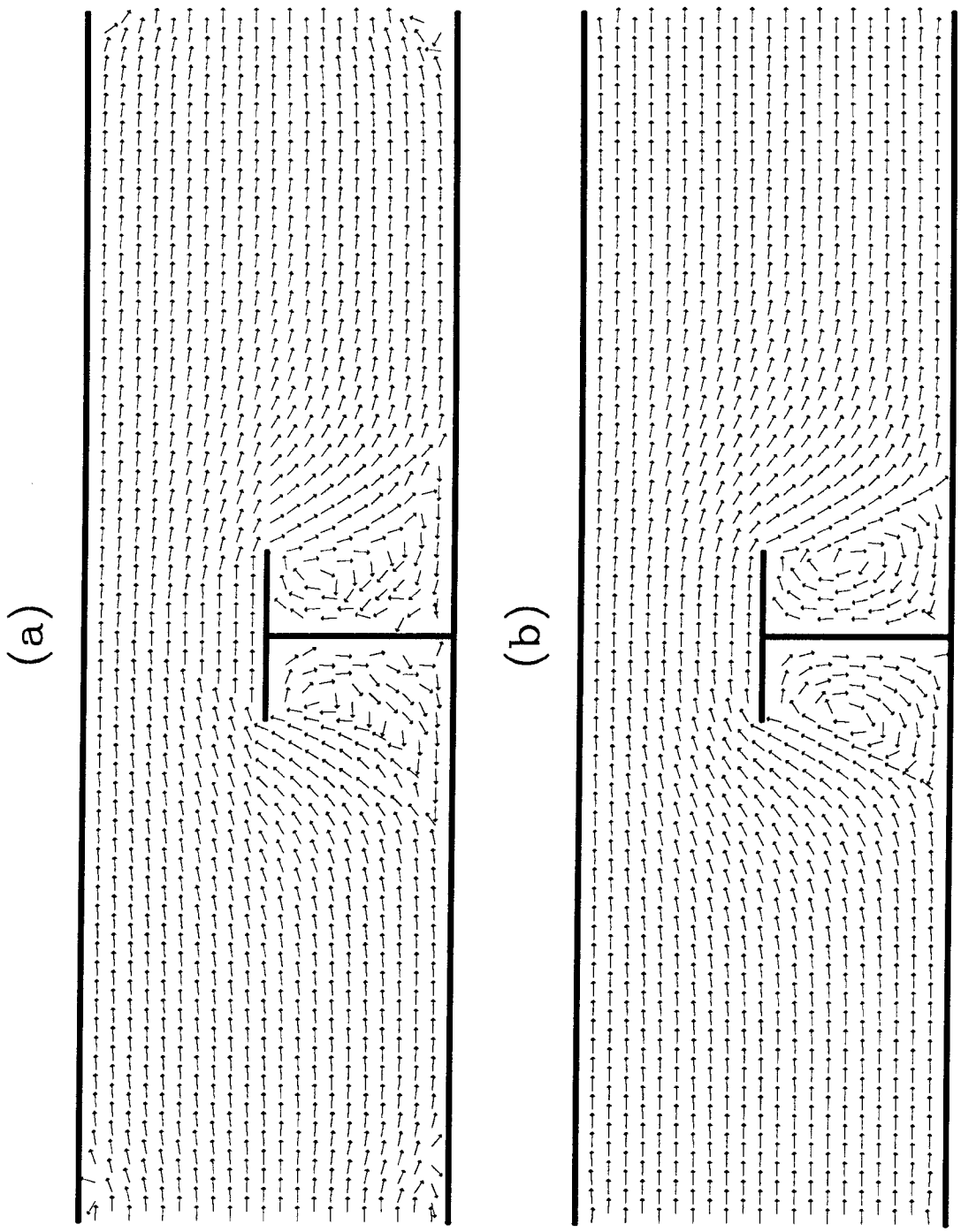

FIG. 6. Velocity field obtained with: (a) the nonlinear model; (b) the linear model. To emphasize the directions of the flow, only the directions of the velocities are plotted. The amplitudes of the arrows are normalized.

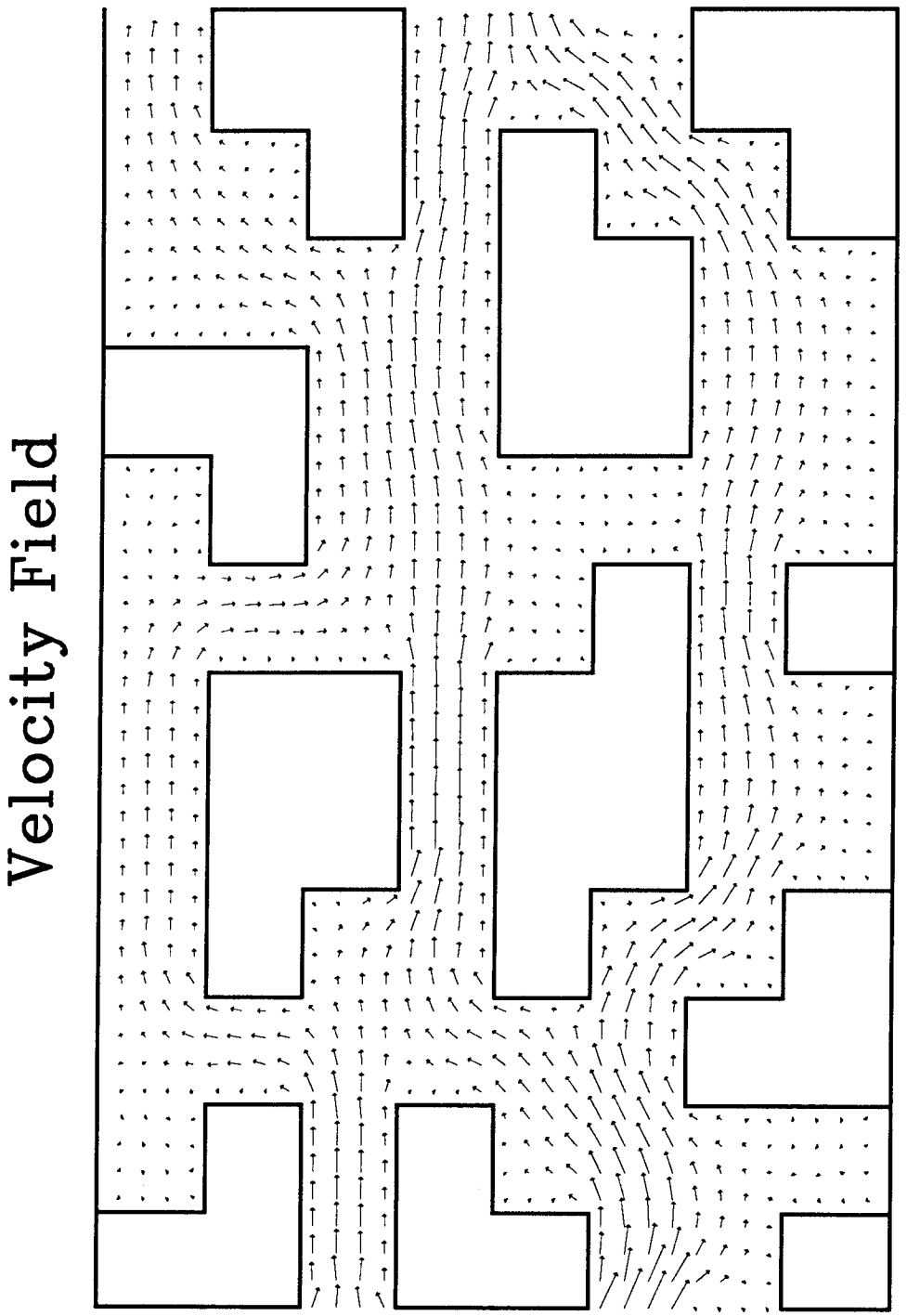

FIG. 7. Velocity field of the fluid flow through a porous medium. At each location, the length of the arrow represents the amplitude of the velocity. The direction of the arrow points to the direction of the flow.